Journal of Organometallic Chemistry 695 (2010) 1972–1978

Contents lists available at ScienceDirect

Journal of Organometallic Chemistry

journal homepage: www.elsevier.com/locate/jorganchem

Pure red electrophosphorescence from polymer light-emitting diodes doped with highly emissive bis-cyclometalated iridium(III) complexes

Hidetaka Tsujimoto [a], Shigeyuki Yagi [a,*], Hotaka Asuka [a], Yuji Inui [a], Shigeru Ikawa [a], Takeshi Maeda [a], Hiroyuki Nakazumi [a], Yoshiaki Sakurai [b]

[a] Department of Applied Chemistry, Graduate School of Engineering, Osaka Prefecture University, 1-1 Gakuen-cho, Naka-ku, Sakai, Osaka 599-8531, Japan
[b] Environment and Chemistry Department, Technology Research Institute of Osaka Prefecture, 2-7-1 Ayumino, Izumi, Osaka 594-1157, Japan

ARTICLE INFO

Article history:
Received 6 February 2010
Received in revised form
8 May 2010
Accepted 10 May 2010
Available online 31 May 2010

Keywords:
Bis-cyclometalated iridium(III) complex
Red phosphorescence
Organic light-emitting diode
Polymer light-emitting diode
Photoluminescence quantum yield

ABSTRACT

In order to develop highly emissive red phosphorescent materials for OLED application, novel bis-cyclometalated iridium(III) complexes were developed using the 1-(dibenzo[*b*,*d*]furan-4-yl)isoquinolinato-*N*,$C^{3'}$ (*dbfiq*) cyclometalating ligand. When 1,3-bis(3,4-dibutoxyphenyl)propane-1,3-dionate (*bdbp*) is employed as an ancillary ligand, Ir(*dbfiq*)$_2$(*bdbp*) **1** exhibits red photoluminescence (PL) at 640 nm with a quantum yield (Φ_{PL}) of 0.61 (in toluene, 298 K). Replacement of *bdbp* to dipivaloylmethanate (*dpm*) and acetylacetonate (*acac*) (Ir(*dbfiq*)$_2$(*dpm*) **2** and Ir(*dbfiq*)$_2$(*acac*) **3**, respectively) does not affect the PL spectrum, but reduces Φ_{PL} to 0.55 and 0.49 for **2** and **3**, respectively. Similar tendency is also found in the doped poly(methyl methacrylate) (PMMA) film, and **1** is more emissive ($\Phi_{PL} = 0.17$) than **2** and **3** ($\Phi_{PL} = 0.08$ and 0.06, respectively). Using **1** as a phosphorescent dopant, polymer light-emitting diodes (PLEDs) were fabricated, of which structure was ITO/PEDOT:PSS (40 nm)/PVCz:**1**:PBD (100 nm)/CsF (1 nm)/Al (250 nm). Pure red electroluminescence (EL) is obtained from the fabricated PLEDs, affording a CIE chromaticity coordinate of (0.68, 0.31). When 0.51 mol% of **1** is incorporated in the PVCz-based emitting layer, the PLED shows maximum luminance of 7270 cd m^{-2} at 16.5 V, power efficiency of 1.4 lm W^{-1} at 7.5 V, and external quantum efficiency of 6.4% at 9.0 V. PLEDs with the same structure and components were also fabricated using **2** and **3**, and their device characteristics were investigated. In proportion to the PL quantum yields, **1** affords better device performance than **2** and **3**. Owing to four butoxy groups introduced to the *bdbp* ligand, **1** exhibits high solubility in organic solvents such as chloroform and toluene, and thus, is an excellent red phosphorescent dopant for solution-processed OLEDs.

1. Introduction

Recent development in organic light-emitting diodes (OLEDs) has brought about considerable progress in electrooptical applications such as self-emitting flat-panel displays and illumination devices [1–5]. The promising strategy to obtain high performance OLEDs is utilization of phosphorescent emitters because they can overcome the limit of quantum efficiency in fluorescent OLEDs [6]. From this viewpoint, phosphorescent organometallic complexes with heavy metal centers have received considerable attention as emitting dopants for OLEDs. Especially, bis- and tris-cyclometalated Ir(III) complexes have been intensely studied, as represented by homoleptic Ir(*C*^*N*)$_3$ [7–10] and heteroleptic Ir(*C*^*N*)$_2$(*O*^*O*) [11,12] complexes (*C*^*N*, 2-arylpyridinate or a related ligand; *O*^*O*, a β-diketonate ligand). In these complexes, strong spin-orbit coupling facilitating intersystem crossing from the singlet excited state to the triplet state leads to high internal quantum efficiency of phosphorescent electroluminescence (EL), up to 100% [13,14]. Thus, numerous amounts of Ir(III)-based phosphorescent emitters for RGB primary colors have so far been developed. However, the development of red phosphorescent Ir(III) complexes with high quantum yields is still difficult because they are intrinsically less emissive than blue and green emitters. Although Ir(*piq*)$_3$ [9] and Ir(*btp*)$_2$(*acac*) [15] are well known as red phosphorescent emitters (*piq* and *btp*; 1-phenylisoquinolinato-*N*,$C^{2'}$ and 2-(2′-benzo[*b*]thienyl)pyridinato-*N*,$C^{3'}$ ligands, respectively), their photoluminescence quantum yields in solution are not more than 0.26. In order to achieve high device performance of red emitting OLEDs, highly emissive red phosphorescent materials are eagerly required.

* Corresponding author. Tel.: +81 72 254 9324; fax: +81 72 254 9910.
E-mail address: yagi@chem.osakafu-u.ac.jp (S. Yagi).

0022-328X/$ – see front matter © 2010 Elsevier B.V. All rights reserved.
doi:10.1016/j.jorganchem.2010.05.011

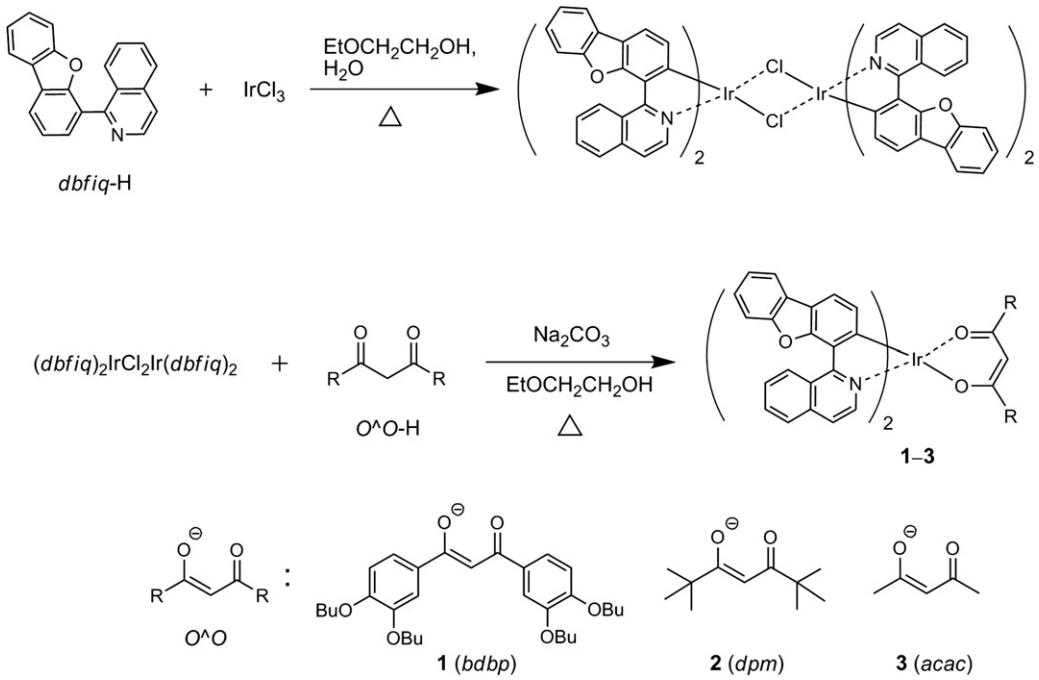

Scheme 1. Synthesis of bis-cyclometalated Ir(III) complexes **1**–**3**.

Another important matter is applicability of phosphorescent organometallic complexes as emitting dopants in solution-processed OLEDs [16]. For fabrication of OLEDs, solution processing methods such as spin-coating and ink-jet printing techniques are intensely investigated because of lots of advantages; efficient use of constituent materials, facile device fabrication with saved electric power, and availability of large-area devices. Thus, from the industrial viewpoint, solution processing is eagerly required rather than vacuum deposition processing, and the achievement of high device performance in solution-processed devices is one of main subjects of development of OLEDs. The phosphorescent organometallic complexes used for OLEDs are, however, often less soluble in organic solvents and host materials used in fabrication of solution-processed OLEDs. With this respect, the development of well-soluble phosphorescent organometallic complexes should provide lots of opportunities to optimize the device performance.

In the present study, we report a novel, highly emissive red phosphorescent Ir(III) complex **1**, composed of two 1-(dibenzo[*b*,*d*]furan-4-yl)isoquinolinato-*N*,$C^{3'}$ (*dbfiq*) cyclometalating ligands and one 1,3-bis(3,4-dibutoxyphenyl)propane-1,3-dionate-*O*,*O* (*bdbp*) ancillary ligand. We expect that the rigid and extended π-conjugation framework of the *dbfiq* ligand should yield pure and saturated red emission with high quantum efficiency. Aimed at solution-processed OLEDs, *bdbp* is employed as a diketonate ancillary ligand to improve the solubility in organic media. Recently, we reported that heteroleptic cycloplatinate(II) complexes with *bdbp* as an ancillary ligand, namely Pt(*C*^*N*)(*bdbp*), exhibited improved solubility in various organic solvents as well as enhanced photoluminescence in comparison with the complexes bearing aliphatic ancillary ligands such as dipivaloylmethanate (*dpm*) and acetylacetonate (*acac*) [17]. We here show the EL performance of the solution-processed polymer light-emitting diode (PLED), using **1** as a red emitting dopant. We also investigate **2** and **3**, the *dpm* and *acac* analogues of **1**, respectively, to elucidate how the *bdbp* ligand affects the PL and EL properties of the *dbfiq*-based bis-cyclometalated iridium(III) complex.

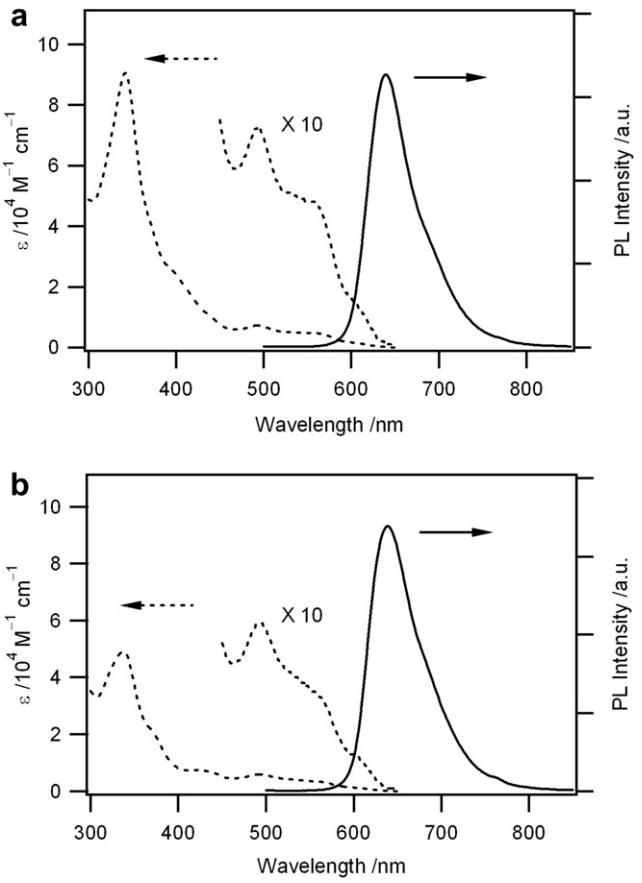

Fig. 1. UV–vis absorption and photoluminescence spectra of **1** (a) and **2** (b) in toluene solutions at 298 K.

Table 1
UV–vis absorption and photoluminescence spectral data of **1**–**3**.

Complex	UV–vis[a,b]		PL in solution[a,c]		PL in PMMA film[e]	
	λ_{abs}/nm (log ϵ)	λ_{PL}/nm	τ_{PL}/μs[d]	Φ_{PL}	λ_{PL}/nm	Φ_{PL}
1	342 (4.96), 494 (3.86)	640	1.07	0.61	635	0.17
2	337 (4.69), 492 (3.77)	639	1.04	0.55	634	0.08
3	336 (4.73), 492 (3.78)	639	0.93	0.49	638	0.06

[a] Obtained in toluene at 298 K.
[b] [Ir complex] = 10 μM.
[c] [Ir complex] = 1.0 μM.
[d] The χ^2 value for each data is 1.000–1.003.
[e] Obtained for 1.5 wt%-doped PMMA spin-coated films (film thickness: *ca.* 100 nm) at ambient temperature.

2. Results and discussion

2.1. Synthesis of red phosphorescent Ir(III) complexes *1*–*3*

The synthesis of Ir(III) complex **1** is shown in Scheme 1. The preparation of diketone *bdbp*-H was previously reported [17]. The cyclometalating ligand *dbfiq*-H was prepared by the Suzuki–Miyaura cross-coupling reaction of commercially available dibenzo[*b*,*d*]furan-4-ylboronic acid and 1-chloroisoquinoline. The obtained *dbfiq*-H was subsequently reacted with $IrCl_3$ to afford a μ-chloro-bridged Ir(III) dimer $(dbfiq)_2Ir(\mu\text{-}Cl)_2Ir(dbfiq)_2$, which was reacted with *bdbp*-H in 2-ethoxyethanol in the presence of Na_2CO_3 to afford **1** [15]. The yield of **1** significantly depended on the reaction time, and the optimization of the reaction time was carried out using an automatic synthesizer to obtain uniform conditions (see Experimental and 4.3). The yield of **1** increased with the increase of the reaction time, and the maximum yield of 55% was obtained at 3 h. Further extension of the reaction time led to the decrease in the yield down to 15% at 24 h. The addition of Ag_2O as a halide absorber was not effective to improve the yield of **1** [18,19]. Under the optimized reaction conditions, the yield of **1** was finally improved up to 60% in a manual way (see Experimental and 4.2.3).

The Ir(III) complexes **2** and **3** with *dpm* and *acac* ancillary ligands, respectively, were prepared as the reference compounds in a similar way to the preparation of **1** (65 and 57% yields for **2** and **3**, respectively, from $(dbfiq)_2Ir(\mu\text{-}Cl)_2Ir(dbfiq)_2$). The structures of **1**, **2** and **3** were identified by ^1H NMR and MALDI-TOF mass spectra as well as elemental analyses. One can see that there are geometric isomers for the structure of the $Ir(C\text{^}N)_2(O\text{^}O)$-type complex. According to the literatures, X-ray crystallographic analyses indicate that *cis*-C,C and *trans*-N,N configuration is more favored for this type of complexes [7,11,20,21]. Although we tried to clarify the configuration of **1**–**3** by X-ray crystallography, suitable single crystals were not obtained. However, the elemental analyses afforded satisfactory data to guarantee the purity of the present Ir(III) complexes, and the ^1H NMR spectrum, showing one signal set, indicated that each complex exists as a single isomer (see Supplementary data).

Table 2
Electrochemical properties of **1**–**3**.

Compd	$E^{ox}_{1/2}$/V[a]	$E^{red}_{1/2}$/V[b]	HOMO/eV[c]	LUMO/eV[c]
1	0.82	−1.62	5.21	2.77
2	0.97	−1.58	5.36	2.81
3	0.93	−1.53	5.32	2.86

[a] The oxidation potential vs. SCE.
[b] The reduction potential vs. SCE.
[c] The HOMO and LUMO levels are represented versus vacuum.

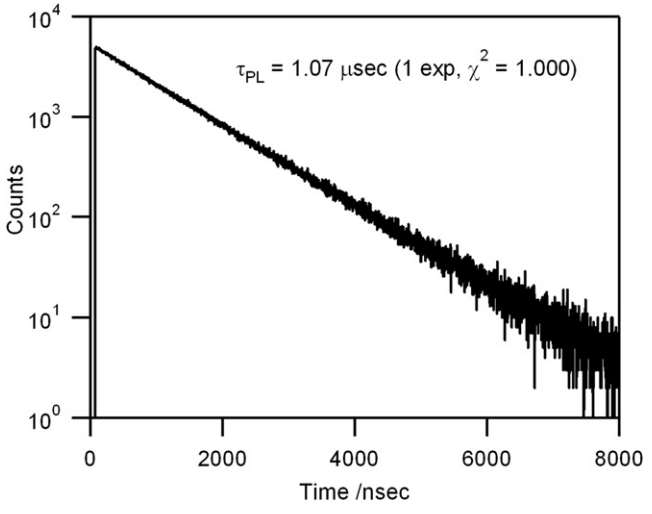

Fig. 2. Time-resolved photoluminescence decay of **1** (1.0 μM) in deaerated toluene at ambient temperature; excitation wavelength, 388 nm. Data were collected for photoluminescence in the region of >550 nm.

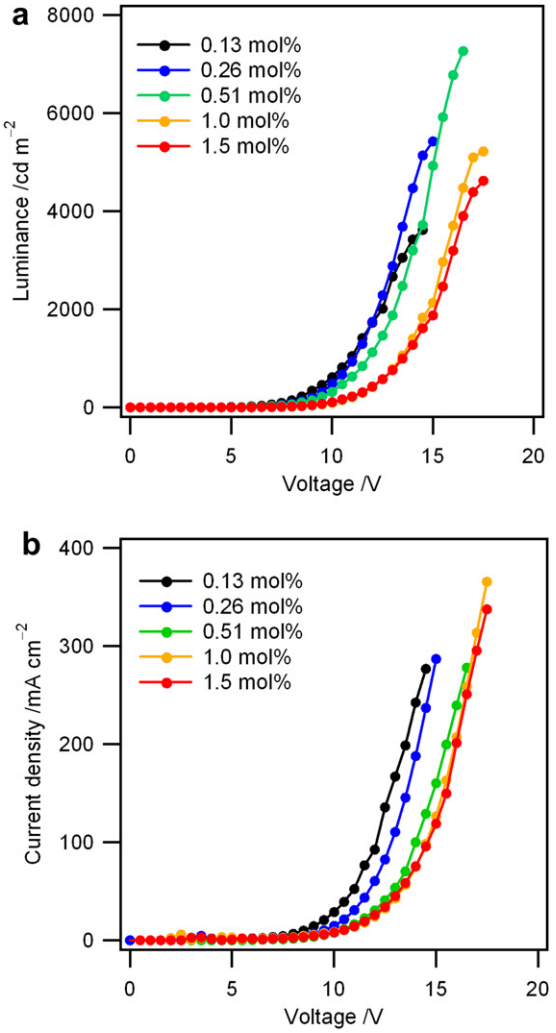

Fig. 3. Luminance–voltage (a) and current density–voltage (b) characteristics of PLEDs containing varying concentrations of **1** (x = 0.13, 0.26, 0.51, 1.0, and 1.5 mol%).

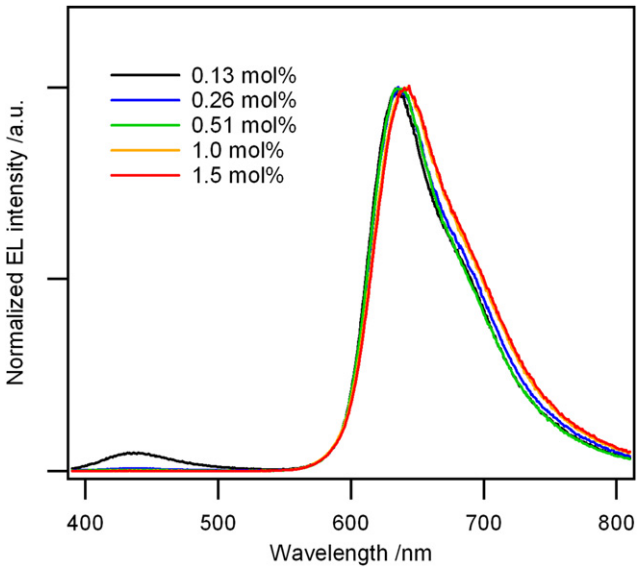

Fig. 4. Normalized electroluminescence spectra from PLEDs containing varying concentrations of **1** ($x = 0.13$, 0.26, 0.51, 1.0, and 1.5 mol%). Each spectrum was obtained at the voltage that provides the maximum luminance.

2.2. UV–vis absorption and photoluminescent properties

In Fig. 1 are shown UV–vis absorption and photoluminescence (PL) spectra of **1** and **2** in toluene at 298 K. The spectral data for **1**–**3** in solutions and polymer matrices are also summarized in Table 1, accompanied by PL quantum yields and PL lifetimes. In the UV–vis spectrum of **1**, strong structured absorption bands at <400 nm are assigned to *C^N* ligand-centered (LC) π–π^* transitions. The next low-energy transitions at 400–500 nm can be assigned to the spin-allowed metal-to-ligand charge transfer (^{1}MLCT). The absorption bands with comparable intensities to the ^{1}MLCT transitions are also observed at 500–600 nm, which are assigned to the spin-forbidden ^{3}MLCT transitions. The relatively large intensities of the ^{3}MLCT transition bands indicate effective mixing of the ^{3}MLCT level with the ^{1}MLCT due to the strong spin-orbit coupling caused by the Ir(III) center [7,15]. In comparison to the spectrum of **1**, the reduced molar absorptivity was obtained in the near-UV region (300–400 nm) for **2**. This spectral difference arises from the intense π–π^* transition in the extensively conjugated *bdbp* ligand of **1** masking the LC (*C^N*) transition bands. The ^{3}MLCT transition band was also observed for **2** in the same region as **1**. The reference complex **3** exhibited a similar absorption spectrum to **2**.

The PL spectrum of **1** was obtained for a deaerated toluene solution, and the λ_{PL} was observed at 640 nm, emitting pure red. As shown in Fig. 2, the PL lifetime of 1.07 μs ($\chi^2 = 1.000$), well fitted to a single-exponential decay, was obtained for **1**, indicating that the observed PL was phosphorescence. Such a short phosphorescence lifetime is effective to suppress triplet–triplet annihilation in phosphorescent OLEDs [22]. The PL spectra of **2** and **3** were almost identical to that of **1**, showing the λ_{PL}s at 639 nm. This indicates that the *O^O* ligand did not significantly affect the λ_{PL}. It is notable that the present red phosphorescent Ir(III) complexes are very emissive: the PL quantum yield (Φ_{PL}) of **1** is 0.61 (in toluene at 298 K), and much more emissive than well-known red phosphorescent materials such as Ir(*piq*)$_3$ (Φ_{PL}; 0.26 in toluene at 298 K) [9] and Ir(*btp*)$_2$(*acac*) (Φ_{PL}; 0.21 in 2-methyltetrahydrofuran at 298 K) [15]. The Φ_{PL}s of **2** and **3** are 0.55 and 0.49 (in toluene at 298 K), respectively, a little smaller than that of **1**. We also investigated the PL properties of **1**–**3** in polymer matrices. The PL spectra of **1**–**3** were obtained for 1.5 wt%-doped poly(methyl methacrylate) (PMMA) thin films, each of which was identical to that obtained in solution. The Φ_{PL}s were significantly reduced to 0.17, 0.08, and 0.06 for **1**–**3**, in comparison to those obtained for the solutions. However, **1** was more emissive than **2** and **3** even in the polymer matrix. Thus, replacing *dpm* and *acac* to *bdbp* is beneficial to enhance phosphorescence quantum efficiency of the present bis-cyclometalated Ir(III) complex system. Also, owing to the *bdbp* ancillary ligand, **1** is very soluble in organic solvents such as toluene and chloroform. For example, the solubility of **1** in toluene is 28 mM, much larger than that of **3** (14 mM). This property is also helpful to tune the concentration of the phosphorescent dopant in a polymer host upon fabrication of PLED.

2.3. Electrochemical properties

In order to determine the HOMO-LUMO band gaps of the Ir(III) complexes, the electrochemical properties were investigated. The cyclic voltammograms were obtained for DMF solutions of **1**–**3** (1.0 mM), using 0.1 M tetrabutylammonium perchlorate as a supporting electrolyte [11,23,24]. The redox potentials were recorded relative to the Ag/AgCl reference electrode with Pt wire used for both working and counter electrodes. Ferrocene (Cp_2Fe) was used as an internal reference ($Cp_2Fe/Cp_2Fe^+ = 0.41$ V vs. SCE in DMF). The complexes **1**–**3** showed reversible oxidation and reduction with half-wave potentials ($E^{ox}_{1/2}$ and $E^{red}_{1/2}$, respectively). The obtained data are summarized in Table 2. The HOMO and LUMO levels were estimated from the oxidation and reduction potentials, respectively, assuming that the HOMO of Cp_2Fe is 4.8 eV versus vacuum. The HOMO of **1**–**3** ranged from 5.21 to 5.36 eV, and the LUMO did from 2.77 to 2.86 eV. Thus, the HOMO and LUMO levels are independent on the diketonate ancillary ligand.

2.4. Electroluminescent properties of PLEDs

Using **1** as a phosphorescent dopant, the PLED based on poly(*N*-vinylcarbazole) (PVCz) was fabricated [25,26]. The configuration of

Table 3
EL device performance of PLED containing **1** as a phosphorescent dopant.

Device[a]	λ_{EL}/nm[b]	L_{max}/cd m^{-2}[c]	η_c/cd A^{-1}[c]	η_p/lm W^{-1}[c]	η_{ext}/%[c]	CIE (x, y)[b]
1 ($x = 0.13$ mol%)	636	3620 (14.5)	2.2 (7.5)	0.93 (7.5)	3.5 (7.5)	(0.63, 0.29)
2 ($x = 0.26$ mol%)	636	5430 (15.0)	2.9 (9.0)	0.99 (8.5)	4.9 (9.0)	(0.68, 0.31)
3 ($x = 0.51$ mol%)	637	7270 (16.5)	3.9 (9.0)	1.4 (7.5)	6.4 (9.0)	(0.68, 0.31)
4 ($x = 1.0$ mol%)	640	5220 (17.5)	1.9 (13.5)	0.45 (11.5)	3.5 (13.5)	(0.69, 0.31)
5 ($x = 1.5$ mol%)	641	4620 (17.5)	1.7 (12.5)	0.47 (10.5)	3.3 (12.5)	(0.69, 0.31)

[a] The emitting layer consists of PVCz, PBD and **1** (PVCz, 84.6–85.8 mol%; PBD, 13.8–14.0 mol%; **1**, x mol%). The molar ratio of PVCz was represented by the concentration of the vinylcarbazole monomer unit.
[b] Obtained at the voltage where the maximum luminance was observed.
[c] The maximum values of luminance (L_{max}), current efficiency (η_c), power efficiency (η_p), and external quantum efficiency (η_{ext}) for the devices. The values in parentheses are the voltages at which they were obtained.

Table 4
EL device performance of PLEDs containing **2** and **3** as a phosphorescent dopant.[a]

Ir complex	λ_{EL}/nm[b]	L_{max}/cd m^{-2}[c]	η_c/cd A^{-1}[c]	η_p/lm W^{-1}[c]	η_{ext}/%[c]	CIE (x, y)[b]
2	636	4109 (16.5)	1.9 (10.5)	0.56 (10.5)	3.3 (10.5)	(0.68, 0.31)
3	639	4575 (16.5)	1.6 (10.5)	0.49 (10.5)	2.9 (10.5)	(0.68, 0.31)

[a] The device structure was the same as that of Device 3 (x = 0.51 mol%) in Table 4.
[b] Obtained at the voltage where the maximum luminance was observed.
[c] The maximum values of luminance (L_{max}), current efficiency (η_c), power efficiency (η_p), and external quantum efficiency (η_{ext}) for the devices. The values in parentheses are the voltages at which they were obtained.

the device is ITO (transparent anode, 150 nm)/PEDOT:PSS (40 nm)/emitting layer (EML, 100 nm)/CsF (1.0 nm)/Al (cathode, 250 nm), where the EML consists of PVCz (84.6–85.7 mol%, based on the vinylcarbazole monomer unit), PBD (13.9–14.0 mol%), and **1** (0.13–1.5 mol%). We especially focused on the concentration of **1** to optimize the ratio of the constituent materials of the EML. The PEDOT:PSS and PVCz emitting layers were successively spin-coated on ITO, and the CsF layer and the Al cathode were placed by the vacuum deposition. In Fig. 3 are shown luminance–voltage (L–V) and current density–voltage (J–V) relationships of the PLED at different concentrations of **1** (x mol%). The EL spectra of the devices are shown in Fig. 4. The device performance is also summarized in Table 3. As the increasing voltage was applied, the electric current emerged at 4.5–6.0 V along with red EL. The emission maximum was slightly red-shifted from 636 to 642 nm when the concentration of **1** increased. This red shift can be explained by excimer formation of **1** that partially contributes to the EL spectrum [11,24,27]. The maximum luminance (L_{max}) was also affected by the concentration of **1**. At x = 0.13 mol%, L_{max} was just 3620 cd m^{-2} at 14.5 V, corresponding to 1.3 cd A^{-1}, and the EL spectra was accompanied with weak emission at 436 nm assigned to the PVCz-PBD exciplex [28], indicating that the excitons of PVCz were not sufficiently consumed for the electrophosphorescence from **1**. The addition of the dopant at the ratio of x = 0.51 mol% led to the increase in L_{max} up to 7270 cd m^{-2} (@16.5 V) corresponding to 2.6 cd A^{-1}. This dopant concentration also afforded better PLED performance; $\eta_{j\ max}$ = 3.9 cd A^{-1} (@9.0 V), $\eta_{p\ max}$ = 1.4 lm W^{-1} (@7.5 V), and $\eta_{ext\ max}$ = 6.4% (@9.0 V). Further doping led to the decrease in L_{max} as well as the device performance. It is worthy to note that the present device exhibits the Commission Internationale de L'Eclairage (CIE) chromaticity coordinate of (0.68, 0.31), shifting to the pure red region over the National Television System Committee (NTSC) standard of red, (0.67, 0.33).

We also prepared PLEDs using the reference complexes **2** and **3**. The device structure was the same as that for **1**, and the concentration of the Ir(III) complex was adjusted to 0.51 mol%. The EL spectra from **2** and **3** were almost identical to that of **1** (λ_{EL} = 639 and 636 nm, respectively), both of which gave the CIE chromaticity coordinate of (0.68, 0.31). The device characteristics are summarized in Table 4 and obviously inferior to PLED containing **1** (see Table 4, x = 0.51 mol%). This tendency corresponds to that for the PL quantum yields in solutions and PMMA films. In Fig. 5 is shown the HOMO/LUMO levels and the triplet energy of the materials used in the present PLED. The HOMO and LUMO levels of **1**–**3** are almost similar to one another and embedded between the HOMO of PVCz (5.80 eV) and the LUMO of PBD (2.40 eV) [29]. Thus, efficient hole and electron transfer to the Ir(III) complex should occur in the emitting layer. Also, as the triplet energy of the iridium complexes (1.94–1.95 eV) are lower than those of PVCz (2.46 eV) [30] and PBD (2.46 eV) [31], the back energy transfer should be suppressed. Taking this into consideration, the PLED performance in luminance should be determined by the intrinsic quantum efficiency of **1**–**3** in radiative decay.

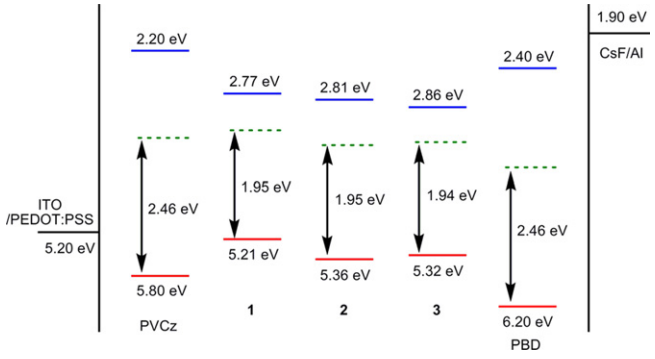

Fig. 5. Energy diagram of the present PLED. The red and blue solid lines represent the HOMO and LUMO levels, respectively, and the green dashed lines represent the T_1 levels (For interpretation of the references to colour in this figure legend, the reader is referred to the web version of this article).

3. Conclusions

In conclusion, we developed novel pure red phosphorescent bis-cyclometalated Ir(III) complexes **1**–**3**, employing *dbfiq C^N* ligand. Although the *O^O* ancillary ligand does not affect the emission wavelength, the employment of the *bdbp* ligand, in place of *acac* and *dpm*, gives rise to the increase in Φ_{PL} up to 0.61 in toluene at 298 K. The *bdbp* ligand enhanced the solubility of the *dbfiq*-based bis-cyclometalated Ir(III) complexes in organic solvents. Using these red phosphorescent complexes as emitters, PVCz-based PLEDs were fabricated. Pure red EL with the CIE chromaticity coordinate of (0.68, 0.31) is obtained from **1**–**3**, and the PLED with **1** shows better performance (L_{max} = 7270 cd m^{-2} at 16.5 V, $\eta_{j\ max}$ = 3.9 cd A^{-1} at 9.0 V, $\eta_{p\ max}$ = 1.4 lm W^{-1} at 7.5 V, $\eta_{exp\ max}$ = 6.4% at 9.0 V), in comparison to those with **2** and **3**. Taking into consideration that the HOMO-LUMO levels and triplet energy of **1**–**3** are similar (HOMO, 5.21–5.36 eV; LUMO, 2.77–2.86 eV; triplet energy, 1.94–1.95 eV), the PLED performance predominantly depends on the phosphorescent quantum efficiency of the emitter. From these results, **1** is an excellent red phosphorescent material for solution-processed OLEDs.

4. Experimental

4.1. General

^{1}H NMR spectra were obtained on a Jeol JNM-LA300 (300 MHz), a Jeol JNM-LA400 (400 MHz), or a Jeol JNM-ECX400 (400 MHz) spectrometer, using TMS as an internal standard (0.00 ppm). Matrix-assisted laser desorption/ionization time-of-flight (MALDI-TOF) mass spectra were measured on a Shimadzu Kratos Compact MALDI 2 using shinapinic acid as a matrix. Elemental analyses were carried out on a Yanako CHN CORDER MT-3 analyzer.

Cyclic voltammograms were recorded on a Hokuto Denko HZ-5000 electrochemical measurement system at a scanning rate of 100 mV/s. The measurements were performed for the Ir(III) complexes in freshly distilled DMF, where 0.1 M tetrabutylammonium perchlorate ($Bu_4N^+ClO_4^-$) was used as a supporting electrolyte. The potentials were recorded relative to a Ag/AgCl reference

electrode with Pt wire used for both working and counter electrodes. Ferrocene was used as an internal reference ($Cp_2Fe/Cp_2Fe^+ = 0.41$ V vs. SCE in DMF).

UV–vis and photoluminescence (PL) spectra were measured on a Shimadzu UV-3100 and a Jasco FP-6600 spectrophotometer, respectively, using a quartz cell. PL lifetimes were obtained on a Horiba Jobin Yvon FluoroCube spectroanalyzer using a 388 nm nanosecond-order LED light source. PL quantum yields were obtained on a Hamamatsu Photonics C9920 PL quantum yield measurement system. The sample solutions for optical and photophysical measurements were deaerated by argon bubbling followed by complete sealing, and the analyses were carried out just after preparation of the samples.

For the preparation of *dbfiq*-H, dibenzo[*b*,*d*]furan-4-ylboronic acid and 1-chloroisoquinoline were purchased from Sigma–Aldrich Co.. As a catalyst for the Suzuki–Miyaura cross-coupling reaction, $Pd(PPh_3)_4$ was purchased from Wako Pure Chemical Industries, Ltd. 1,2-Dimethoxyethane was purchased from Wako Pure Chemical Industries, Ltd. For the preparation of **1**–**3**, 2-ethoxyethanol was purchased from Wako Pure Chemical Industries, Ltd and used as freshly opened. The preparation of 1,3-bis(3,4-dibutoxyphenyl) propane-1,3-dione (*bdbp*-H) was previously reported [17].

For fabrication of PLEDs, poly(*N*-vinylcarbazole) (PVCz, $M_w = 25{,}000–50{,}000$) was purchased from Sigma–Aldrich Co., and used after purification by reprecipitation from THF to methanol. Poly(3,4-ethylenedioxythiophene):poly(styrenesulfonate) (PEDOT:PSS, Clevios P VP AI.4083) was purchased from G.H. Starck Clevios GmbH, and 2-(4-biphenylyl)-5-(4-*tert*-butylphenyl-1,3,4-oxadiazole) (PBD) was purchased from Tokyo Chemical Industry Co., Ltd. Cesium fluoride and Al wires were purchased from Wako Pure Chemical Industries, Ltd and The Nilaco Corporation, respectively. Pre-patterned indium-tin-oxide (ITO, 150 nm thickness) glass substrates with sheet resistance of *ca.* 10 Ω/□ were purchased from Sanyo Vacuum Industries Co., Ltd.

4.2. Preparation of materials

4.2.1. Preparation of 1-(dibenzo[b,d]furan-4-yl)isoquinoline (dbfiq-H)

To a mixture of 1-chloroisoquinoline (1.74 g, 10.1 mmol) and $Pd(PPh_3)_4$ (403 mg, 0.349 mmol) in 1,2-dimethoxyethane (50 mL) were added a solution of dibenzofuran-4-ylboronic acid (2.30 g, 10.9 mmol) in ethanol (50 mL), followed by addition of 2.6 M sodium carbonate (50 mL). Then, the mixture was heated at reflux for 19 h under nitrogen. After cooling, ethyl acetate (50 mL) and water (100 mL) were added, and the insoluble materials were removed by filtration. The filtrate was divided into two layers, and the upper organic layer was separated using a separation funnel. The lower was extracted with ethyl acetate (30 mL × 2), and all the organic layers were combined, washed with water (100 mL × 3) and sat. brine (100 mL), and dried over anhydrous Na_2SO_4. The solvent was removed on a rotary evaporator, and the residue was purified by silica gel column chromatography using chloroform as eluent to afford a yellow solid. Recrystallization from chloroform–hexane gave a white crystal of the titled compound in 73% yield (2.19 g, 7.43 mmol); ^{1}H NMR (400 MHz, $CDCl_3$) δ 7.35–7.39 (m, 1H), 7.42–7.44 (m, 2H), 7.48–7.56 (m, 2H), 7.69–7.75 (m, 2H), 7.78 (d, $J = 7.8$ Hz, 1H), 7.84 (dd, $J = 0.9$ and 8.7 Hz, 1H), 7.95 (d, $J = 8.7$ Hz, 1H), 8.03 (dd, $J = 1.5$ and 7.8 Hz, 1H), 8.12 (dd, $J = 1.5$ Hz and 7.8 Hz, 1H), 8.73 (d, $J = 5.9$ Hz, 1H); MALDI-TOF MS *m*/*z* 296 ($[M + H]^+$). Anal. Calcd for $C_{21}H_{13}NO$: C 85.40; H 4.44, N 4.74, Found: C 85.26; H 4.64, N 4.70.

4.2.2. Preparation of $(dbfiq)_2Ir(\mu\text{-}Cl)_2Ir(dbfiq)_2$

This compound was prepared according to the conventional procedure [11,32]. To a solution of *dbfiq*-H (1.25 g, 4.32 mmol) in 2-ethoxyethanol (83 mL) was added a solution of $IrCl_3 \cdot 3H_2O$ (740 mg, 2.10 mmol) in water (27 mL), and the mixture was heated on the oil bath for 24 h, where the bath temperature was kept at 105 °C. After cooling, water (400 mL) was added, and the precipitate was collected by filtration. The obtained precipitate was washed with ethanol (100 mL) and hexane (100 mL) to obtain the titled compound as a red solid (1.45 g, 0.89 mmol, 85%). This material was highly insoluble, and thus, used in the next reaction without further purification.

4.2.3. Preparation of bis[1-(dibenzo[b,d]furan-4-yl)isoquinolinato-N,C$^{3'}$]iridium(III) [1,3-bis(3,4-dibutoxyphenyl)propane-1,3-dionate-O,O] (**1**)

A mixture of $(dbfiq)_2Ir(\mu\text{-}Cl)_2Ir(dbfiq)_2$ (500 mg, 0.306 mmol), *bdbp*-H (512 mg, 1.00 mmol) and Na_2CO_3 (200 mg, 1.89 mmol) in ethoxyethanol (40 mL) was heated at 130 °C for 3 h under nitrogen. After cooling, the reaction mixture was poured into water (200 mL) and extracted by chloroform (150 mL × 2). The organic layer was combined and washed sat. brine (300 mL × 3), and then dried over anhydrous Na_2SO_4. The solvent was removed on a rotary evaporator, and the residue was purified by silica gel column chromatography using chloroform as eluent. Further purification was carried out by recrystallization from hexane/ethanol to obtain **1** as a red powder (475 mg, 0.367 mmol, 60%); ^{1}H NMR (400 MHz, $CDCl_3$) δ 0.76 (t, $J = 7.6$ Hz, 6H), 0.91 (t, $J = 7.6$ Hz, 6H), 1.15–1.24 (m, 4H), 1.37–1.55 (m, 8H), 1.68–1.75 (m, 4H), 3.49–3.67 (m, 4H), 3.93 (t, $J = 6.6$ Hz, 4H), 6.44–6.46 (m, 3H), 6.69 (d, $J = 8.3$ Hz, 2H), 7.11 (d, $J = 1.8$ Hz, 2H), 7.21–7.36 (m, 8H), 7.49 (d, $J = 8.3$ Hz, 2H), 7.53 (d, $J = 6.3$ Hz, 2H), 7.70–7.79 (m, 6H), 7.92 (d, $J = 7.6$ Hz, 2H), 8.58 (d, $J = 6.3$ Hz, 2H), 9.12 (d, $J = 8.3$ Hz, 2H); MALDI-TOF MS *m*/*z* 1292 ($[M]^+$). Anal. Calcd for $C_{73}H_{67}IrN_2O_8$: C 67.83; H 5.22, N 2.17, Found: C 67.80; H 5.27, N 2.12.

4.2.4. Preparation of bis[1-(dibenzo[b,d]furan-4-yl)isoquinolinato-N,C$^{3'}$]iridium(III) (2,2,6,6-tetramethylheptane-3,5-dionate-O,O) (**2**)

A mixture of $(dbfiq)_2Ir(\mu\text{-}Cl)_2Ir(dbfiq)_2$ (200 mg, 0.123 mmol), dipivaloylmethane (50.0 mg, 0.271 mmol) and Na_2CO_3 (100 mg, 0.720 mmol) in 2-ethoxyethanol (40 mL) was heated at 130 °C for 1.5 h under nitrogen. After cooling, water (150 mL) was added, and the precipitate was collected by filtration. The obtained solid was dissolved in chloroform, and the organic was washed with water (100 mL × 2) and sat. brine (100 mL), and then dried over anhydrous Na_2SO_4. The solvent was removed on a rotary evaporator, and the residue was purified by alumina column chromatography using dichloromethane as eluent to obtain **2** as a red powder (153 mg, 0.159 mmol, 65%); ^{1}H NMR (400 MHz, $CDCl_3$) δ 0.76 (s, 18H), 5.40, (s, 1H), 6.52 (d, $J = 7.9$ Hz, 2H), 7.20–7.35 (m, 6H), 7.49 (d, $J = 7.9$ Hz, 2H), 7.54 (d, $J = 6.2$ Hz, 2H), 7.70–7.81 (m, 6H), 7.94 (d, $J = 7.9$ Hz, 2H), 8.37 (d, $J = 6.2$ Hz, 2H), 9.14 (d, $J = 8.4$ Hz, 2H); MALDI-TOF MS *m*/*z* 964 ($[M]^+$). Anal. Calcd for $C_{53}H_{43}IrN_2O_4$: C 66.02; H 4.50, N 2.91. Found: C 65.66; H 4.69, N 2.82.

4.2.5. Preparation of bis[1-(dibenzo[b,d]furan-4-yl)isoquinolinato-N,C$^{3'}$]iridium(III) (pentane-2,4-dionate-O,O) (**3**)

A mixture of $(dbfiq)_2Ir(\mu\text{-}Cl)_2Ir(dbfiq)_2$ (210 mg, 0.129 mmol), acetylacetone (29.0 mg, 0.284 mmol) and Na_2CO_3 (105 mg, 0.991 mmol) in 2-ethoxyethanol (40 mL) was stirred at 130 °C for 3 h under nitrogen. After cooling, chloroform (200 mL) was added, and the organic layer was washed with water (200 mL × 3) and sat. brine (200 mL), and then dried over anhydrous Na_2SO_4. The solvent was removed on a rotary evaporator, and the red compound was obtained. And recrystallization from hexane/ethanol gave a red powder of **3** in 57% yield (129 mg, 0.147 mmol); ^{1}H NMR (400 MHz, $CDCl_3$) δ 1.74 (s, 6H), 5.21 (s, 1H), 6.37 (d, $J = 7.8$ Hz, 2H), 7.19–7.34 (m, 6H), 7.47 (d, $J = 8.4$ Hz, 2H), 7.63 (d, $J = 6.0$ Hz, 2H), 7.70–7.84 (m, 6H), 7.98 (d, $J = 7.3$ Hz, 2H), 8.50 (d, $J = 6.3$ Hz, 2H), 9.12 (d,

J = 8.4 Hz, 2H); MALDI-TOF MS m/z 880 ([M]$^+$). Anal. Calcd for $C_{47}H_{31}IrN_2O_4 \cdot 2H_2O$: C 61.63; H 3.85, N 3.06. Found: C 61.72; H 3.58, N 3.13.

4.3. Optimization of preparation of **1**

The investigation of optimized reaction time for the preparation of **1** was carried out using Metler Malti-Max 750 automatic synthesizer. A mixture of (*dbfiq*)$_2$Ir(μ-Cl)$_2$Ir(*dbfiq*)$_2$ (200 mg, 0.123 mmol), *bdbp*-H (188 mg, 0.368 mmol), and Na_2CO_3 (130 mg, 1.23 mmol) in 2-ethoxyethanol (40 mL) was heated to 130 °C over 30 min, and the reaction mixture was kept at the same temperature for 1–24 h. Thereafter, the temperature was lowered dawn to 25 °C over 30 min. These reaction schedules were automatically controlled. The reaction vessels were connected to N_2 lines, and the reaction mixtures were exposed to N_2 streams during the entire reaction process. The workup and purification of the reaction mixture were carried out by CH_2Cl_2–water extraction followed by alumina column chromatography (chloroform as eluent). The yield for each reaction time is as follows; 30, 55, 42, 32, 20, and 15% for 1, 3, 6, 9, 14, and 24 h, respectively.

4.4. Fabrication of PLEDs

The pre-patterned ITO glass substrate was routinely cleaned by ultrasonic treatment in detergent solution, distilled water, methanol, acetone, chloroform, and hexane, and then treated in boiled 2-propanol, followed by drying with gentle flow of dry air. PEDOT:PSS (40 nm) was spin-coated on the ITO layer pre-treated with UV-O_3, and then dried at 120 °C for 30 min under Ar. For fabrication of EML, a mixture of PVCz, PBD, and the Ir(III) complex in toluene (PVCz; 10 mg/0.7 mL of toluene) was filtered through a 0.2 μm Millex-FG filter (Millipore Co.). Then, this stock solution was spin-coated onto the PEDOT:PSS layer under Ar. As the complexes **1**–**3** are different in molecular weight, the ratio of the components of EML was defined by molar percentage, where the concentration of PVCz was represented by the vinylcarbazole unit. The fabricated EML contained 84.6–85.8 mol% of the vinylcarbazole unit, 13.8–14.0 mol% of PBD, and 0.13–1.5 mol% of Ir(III) complex. Thereafter, CsF (1.0 nm) and Al (250 nm) layers were successively deposited onto the organic layers by vacuum deposition with a base pressure of *ca.* 10^{-4} Pa. Finally, the device was covered with a glass cap and encapsulated by a UV-curing epoxy resin under argon atmosphere to prevent oxidation of the cathode and the organic layer. The area of the emitting part was 10 mm^2. All the device fabrication was carried out in a glove box filled with dry argon. The configuration of PLED was ITO (anode)/PEDOT:PSS (40 nm)/PVCz:PBD:Ir(III) complex (100 nm)/CsF (1.0 nm)/Al (cathode, 250 nm).

Acknowledgement

The authors express their thanks to Horiba, Ltd for helpful advice in the photoluminescence lifetime measurement.

Appendix. Supplementary data

Supplementary data associated with this article can be found in the online version, at doi:10.1016/j.jorganchem.2010.05.11.

References

[1] X. Gong, D. Moses, A.J. Heeger, Polymer-based light-emitting diodes (PLEDs) and displays fabricated from arrays of PLEDs. in: K. Müllen, U. Scherf (Eds.), Organic Light-Emitting Devices. Wiley-VCH, Weinheim, 2006, pp. 151–180.
[2] Y. Xiong, W. Xu, C. Li, B. Liang, L. Zhao, J. Peng, Y. Cao, J. Wang, Org. Electron. 9 (2008) 533–538.
[3] S. Reineke, F. Lindner, G. Schwartz, N. Seidler, K. Walzer, B. Lüssem, K. Leo, Nature 459 (2009) 234–239.
[4] X.Y. Zheng, W.Q. Zhu, Y.Z. Wu, X.Y. Jiang, R.G. Sun, Z.L. Zhang, S.H. Xu, Displays 24 (2003) 121–124.
[5] X.-Y. Jiang, Z.-L. Zhang, J. Cao, M. Khan, K. Haq, W.-Q. Zhu, J. Phys. D: Appl. Phys. 40 (2007) 5553–5557.
[6] H. Yersin, W.J. Finkenzeller, Triplet emitters for organic light-emitting diodes: basic properties. in: H. Yersin (Ed.), Highly Efficient OLEDs with Phosphorescent Materials. Wiley-VCH, Weinheim, 2008, pp. 1–97.
[7] A.B. Tamayo, B.D. Alleyne, P.I. Djurovich, S. Lamansky, I. Tsyba, N.N. Ho, R. Bau, M.E. Thompson, J. Am. Chem. Soc. 125 (2003) 7377–7387.
[8] K. Goushi, R. Kwong, J.J. Brown, H. Sasabe, C. Adachi, J. Appl. Phys. 95 (2004) 7798–7802.
[9] A. Tsuboyama, H. Iwawaki, M. Furugori, T. Mukaide, J. Kamatani, S. Igawa, T. Moriyama, S. Miura, T. Takiguchi, S. Okada, M. Hoshino, K. Ueno, J. Am. Chem. Soc. 125 (2003) 12971–12979.
[10] S.J. Lee, K.-M. Park, K. Yang, Y. Kang, Inorg. Chem. 48 (2009) 1030–1037.
[11] S. Lamansky, P. Djurovich, D. Murphy, F. Abdel-Razzaq, R. Kwong, I. Tsyba, M. Bortz, B. Mui, R. Bau, M.E. Thompson, Inorg. Chem. 40 (2001) 1704–1711.
[12] L. Chen, H. You, C. Yang, X. Zhang, J. Qin, D. Ma, J. Mater. Chem. 16 (2006) 3332–3339.
[13] C. Adachi, M.A. Baldo, M.E. Thompson, S.R. Forrest, J. Appl. Phys. 90 (2001) 5048–5051.
[14] C. Adachi, M.A. Baldo, S.R. Forrest, M.E. Thompson, Appl. Phys. Lett. 77 (2000) 904–906.
[15] S. Lamansky, P. Djurovich, D. Murphy, F. Abdel-Razzaq, H.-E. Lee, C. Adachi, P. E. Burrows, B. Mui, S.R. Forrest, M.E. Thompson, J. Am. Chem. Soc. 40 (2001) 4304–4312.
[16] A. van Diken, K. Brunner, H. Börner, B.M.W. Langeveld, Highly efficiency phosphorescent polymer LEDs. in: H. Yersin (Ed.), Highly Efficient OLEDs with Phosphorescent Materials. Wiley-VCH, Weinheim, 2008, pp. 311–328.
[17] H. Tsujimoto, S. Yagi, Y. Honda, H. Terao, T. Maeda, H. Nakazumi, Y. Sakurai, J. Lumin. 130 (2010) 217–221.
[18] S.W. Thomas III, S. Yagi, T.M. Swager, J. Mater. Chem. 15 (2005) 2829–2835.
[19] H.-C. Böttcher, M. Graf, H. Krüger, C. Wagner, Inorg. Chem. Commun. 8 (2005) 278–280.
[20] L. Shen, Z. Chen, Q. Zhao, F.-Y. Li, T. Yi, Y. Cao, C.-H. Huang, Inorg. Chem. Commun. 9 (2006) 620–623.
[21] J. Ding, J. Gao, Q. Fu, Y. Cheng, D. Ma, L. Wang, Synth. Met. 155 (2005) 539–548.
[22] C. Adachi, R. Kwong, S.R. Forrest, Org. Electron. 2 (2001) 37–43.
[23] K. Zhang, Z. Chen, C. Yang, Y. Zou, S. Gong, Y. Yao, J. Qin, Y. Cao, J. Mater. Chem. 18 (2008) 3366–3375.
[24] D. Kolosov, V. Adamovich, P. Djurovich, M.E. Thompson, C. Adachi, J. Am. Chem. Soc. 124 (2002) 9945–9954.
[25] M.J. Yang, T. Tsutsui, Jpn. J. Appl. Phys., Part 2 39 (2000) L828–829.
[26] C.-L. Lee, K.B. Lee, J.-J. Kim, Appl. Phys. Lett. 77 (2000) 2280–2282.
[27] G. Zhang, H.-H. Chou, X. Jiang, P. Sun, C.-H. Chen, Y. Ooyama, Y. Harima, Org. Electron. 11 (2010) 632–640.
[28] X. Jiang, R.A. Register, K.A. Killeen, M.E. Thompson, F. Pschenitzka, T.R. Hebner, J.C. Sturm, J. Appl. Phys. 91 (2002) 6717–6724.
[29] M.-H. Kim, M.C. Suh, J.H. Kwon, B.D. Chin, Thin Solid Films 515 (2007) 4011–4015.
[30] Y.-Y. Noh, C.-L. Lee, J.-J. Kim, K. Yase, J. Chem. Phys. 118 (2003) 2853–2864.
[31] M. Suzuki, S. Tokito, F. Sato, T. Igarashi, K. Kondo, T. Koyama, T. Yamaguchi, Appl. Phys. Lett. 86 (2005) 103507–103509.
[32] M. Nonoyama, Bull. Chem. Soc. Jpn. 47 (1974) 767–768.